Application and potential of hydraulic-fracturing for geothermal energy production

Autor(en): **Jung, Reinhard**

Objekttyp: **Article**

Zeitschrift: **Swiss bulletin für angewandte Geologie = Swiss bulletin pour la géologie appliquée = Swiss bulletin per la geologia applicata = Swiss bulletin for applied geology**

Band (Jahr): **19 (2014)**

Heft 2

PDF erstellt am: **24.09.2024**

Persistenter Link: https://doi.org/10.5169/seals-583922

Swiss Bull. angew. Geol. Vol. 19/2, 2014 S. 19-37

Application and potential of hydraulic-fracturing for geothermal energy production

Reinhard Jung[1]

Key words: Hot-Dry-Rock (HDR), Enhanced-Geothermal-Systems (EGS), Hydraulic-Stimulation, Multi-frac-Systems, Waterfrac-Technique

Zusammenfassung

Das grösste Hindernis für die breite Nutzung geothermischer Energie ist die geringe Permeabilität der Tiefengesteine. Dem Hydraulic-Fracturing kommt deshalb eine Schlüsselrolle bei der Erschliessung des riesigen vor allem im kristallinen Grundgebirge gelegenen Potenzials zu. Obwohl seit 1970 ein Dutzend HDR- bzw. EGS-Projekte ausgeführt wurden, ist die Technik nicht ausgereift. Ihre Weiterentwicklung wird derzeit durch die Furcht der Bevölkerung vor induzierter Seismizität behindert. Eine Analyse der Projektergebnisse zeigt, dass die Hauptursache für den schleppenden Fortschritt das Erschliessungskonzept ist, das seit Mitte der 1980er Jahre angewandt wird. Das bis dahin favorisierte Multiriss-Konzept sah vor, zwei geneigte Bohrungen mittels künstlicher Risse zu verbinden. Dieses Konzept wurde nicht zuletzt wegen technischer Schwierigkeiten durch das EGS-Konzept ersetzt. Dieses sieht vor, das natürliche Kluftnetz durch hydraulische Stimulation aufzuweiten. Die Projektergebnisse zeigen jedoch, dass sich stattdessen grosse Einzelrisse ausbilden, bestehend aus natürlichen und künstlichen Risselementen. Aufgrund ihrer Grösse und Eigenschaften bergen diese Makro-Risse ein seismisches Risiko. Mit kleineren Abmessungen aber wären sie aufgrund ihrer hydraulischen Eigenschaften für Multiriss-Systeme gut geeignet. Eine Rückkehr zum Ausgangskonzept ist deshalb angeraten. Multiriss-Konzepte werden in den Schiefergas-Projekten erfolgreich eingesetzt und die Technik hat in den letzten 20 Jahren grosse Fortschritte gemacht. Es ist daher wahrscheinlich, dass auch geothermische Multiriss-Konzepte in naher Zukunft realisiert werden können.

Abstract

The main obstacle for a wide application of geothermal energy is the low permeability of the rock at great depth. Hydraulic-fracturing is therefore the key for exploiting this huge resource located predominantly in the crystalline basement. A dozen projects have been performed since 1970. But still the technique, known as HDR- or EGS-technology is not mature. In addition development is now hindered by the risk of induced earthquakes. A review of the projects shows that the poor progress is mainly due to the exploitation concept applied since the early 1980ties. Until then the leading concept was to connect two inclined boreholes by a set of hydraulic fractures. This multi-fracture scheme was abandoned not the least for technical reasons and replaced by the EGS-concept. This intends to enhance the permeability of the joint network by massive water injection. The results of the EGS-projects however show that this is not happening but that a single macro-fracture is created consisting of natural and new tensile fracture elements. Due to their enormous size and their specific properties they bear a seismic risk. Macro-fractures of a smaller scale are less critical and their hydraulic properties are sufficient for multi-fracture systems. These findings suggest a return to the original HDR-concept. Multi-fracture concepts are applied with great success in shale-gas reservoirs and the techniques to establish these systems have improved considerably. So it seems likely that geothermal multi-fracture systems can be realized in the near future.

[1] JUNG-GEOTHERM UG, Gottfried-Buhr-Weg 19, 30916 Isernhagen, Germany

1 Introduction

Today, geothermal energy production for direct use and/or power production is restricted to hydro-thermal resources. These are intensely fractured, karstified or highly porous rock-formations with extraordinarily high permeabilty. Hydro-thermal resources particularly those suitable for power production are rare especially in countries with normal temperature gradients, where one has to drill deep to reach sufficiently high temperatures. The overwhelming part of the heat content of the upper crust accessible by drilling is stored in rock formations with extremely low permeability, particularly in the crystalline basement. The power potential of these petro-thermal resources is by far the biggest energy resource of the upper crust exceeding the power potential of the hydro-thermal and of all hydro-carbon resources by at least two orders of magnitude.

First attempts to access this potential date back to the early 1970s (Brown et al. 2012). The basic idea is to create large fracture systems in the crystalline rock mass in order to hydraulically connect boreholes over great distances. For power production cold water or natural brine injected in one of the wells heats-up to rock temperature while circulating through the fracture system and is produced in the second well. To prevent flashing an overpressure is maintained in the geothermal loop. Steam for power generation is produced in a secondary loop generally filled with an organic fluid (ORC-Process) or with an ammonia-water mixture (Kalina-Process) as working fluids.

Industrial doublet-systems will have to be designed for an electrical power output of 5–10 MWe and production flow rates in the range of 100 l/s. To ensure a service life of at least 25 years a separation distance of at 0.5 to 2 km between the two wells at depth and a total fracture area of 5–10 km^2 is required. The volume of rock to be accessed by the fracture system has to be in the order of 0.1 to 0.3 km^3. The pumping-power to maintain the geothermal loop can consume a significant fraction of the produced power. For this reason the flow impedance of the fracture system (difference between inlet- and outlet-pressure divided by the flow rate) should not exceed 0.1 MPa/(l/s).

Two concepts had been invented and tested during 40 years of research.

The first regarded the crystalline basement

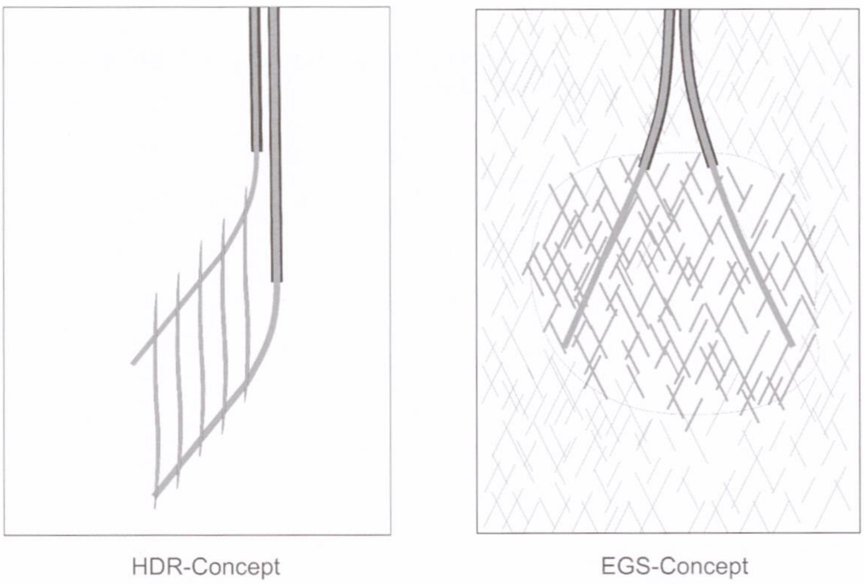

Fig. 1: Basic concepts.

as a competent unfractured rock mass and the idea was to connect two inclined bore-holes by a number of parallel tensile fractures created by hydraulic-fracturing (Fig. 1). The feasibility of this concept, known as Hot-Dry-Rock-concept (HDR), was proofed by creating and investigating single fracture systems at several locations. Attempts to connect two inclined bore-holes by a multi-fracture system in the Los Alamos-project however failed since the fractures did not propagate in the projected direction and due to technical problems with borehole packers at high temperatures (Rowley et al. 1983, Dreesen & Nichol-son 1985, Brown et al. 2012).

Realizing that the crystalline basement contained unsealed natural fractures even at great depth, and that these fractures started to shear before the fluid-pressure reached the level for tensile fracture initiation, the HDR-Concept was abandoned and replaced by the EGS-Concept (Enhanced Geothermal Systems). This concept aims to shear and dilate the natural fracture network by injecting large quantities of water in long uncased borehole sections (Batchelor 1982). In order to distinguish it from hydraulic-fracturing this mechanism was called «hydraulic stimulation» (Murphy 1985). The circulation system is completed by drilling a second borehole into the region of enhanced fracture-permeability (Fig. 1), as indicated by the spatial distribution of seismic events induced during the stimulation process.

The change in the leading concept had severe consequences:

- Deviated or horizontal wells were no longer required and replaced by more or less vertical wells.
- Development of high temperature packers was no longer important and was disregarded.
- Heat exchanging area as a measure for the service life of a HDR-system was replaced by the stimulated rock volume.
- Geometrically simple fracture mechanical models were replaced by geometrically complex fracture networks lacking fracture mechanical mechanisms.

All projects of the last 30 years followed this concept and fracture systems of enormous dimensions (several square-kilometres) had been created during this period connecting boreholes over distances of up to 700 m. Nevertheless, in several aspects the economic targets defined above have not been met. In particular the flow rates and the power output are still far too low (Tab. 1). The main reason is the high flow-impedance

Project	Average Depth	Temp.	Well distance	Flow rate	Flow impedance	Thermal power	Electric power
	[m]	[°C]	[m]	[l/s]	[MPa·s/L]	[MW_{th}]	[MW_{el}]
Los Alamos I	2.840	190	80	6	1.6	2.9	0.4
Los Alamos II	3.500	230	150	6	2.1	3.8	0.5
Camborne II	2.300	80	250	15	0.6	0.6	n.a.
Hijiori II	2.250	250	90	4	0.6	2.9	0.4
Ogachi	850	240	80	1.7	8	1.2	0.16
Soultz I	3.200	170	450	25	0.23	10	1.2
Soultz II	4.700	200	600	12	0.25	6	0.8
Cooper Basin	4.400	250	700	19	1.8	14	1.9
Target		> 150	> 500	100	0.1	> 40	> 5

Tab. 1: Key-parameters of the major EGS-projects.

in the fracture systems. It will be shown in the next chapters that mainly the change of concept is responsible for the poor progress during the last three decades and that a return to the multifracture-concept as envisaged during the first decade of HDR-research and practiced in the shale gas industry is necessary.

2 Test Performance

2.1 Overview

Nine research projects and three commercial HDR-projects have been performed since the beginning of Hot Dry Rock research at around 1970 (Fig. 2). Some of the early projects investigated fracture propagation and fracture properties at shallow depth in order to gain basic knowledge under well-defined but down-scaled conditions, i. e. Le Mayet de Montagne (Cornet 1989), Falkenberg (Jung 1989), Higashihachimantai (Hayashi & Abé 1989) and Fjällbacka (Wallroth 1992). The majority of the projects however were carried out at greater depth under conditions and on a scale similar to future industrial systems (MIT 2006). All together more than a billion Euro have been spent in national and international projects. About 20 deep wells with a total length of about 70 km had been drilled and numerous massive waterfrac-tests including pre- and post-frac investigations had been performed at the different locations. The following paragraphs are an attempt to describe and synthesize the main observations and results of these tests.

Almost all stimulation tests of the EGS-projects had been performed with water or brine as frac-fluid. Only in a few cases viscous-gels and proppants had been used. All tests were done in open-hole sections with lengths ranging from about 10 m up to about 700 m. Generally these intervals particularly those with greater lengths contained hundreds of joints, a number of fracture-zones and faults. In addition they comprised long sections with axial or inclined drilling induced fractures and sections with borehole break-outs. Almost all open-hole sections except those in the Fenton-Hill II and the Camborne System were vertical or sub-vertical. The majority of the stimulation tests were performed with only moderate flow rates, ranging from less

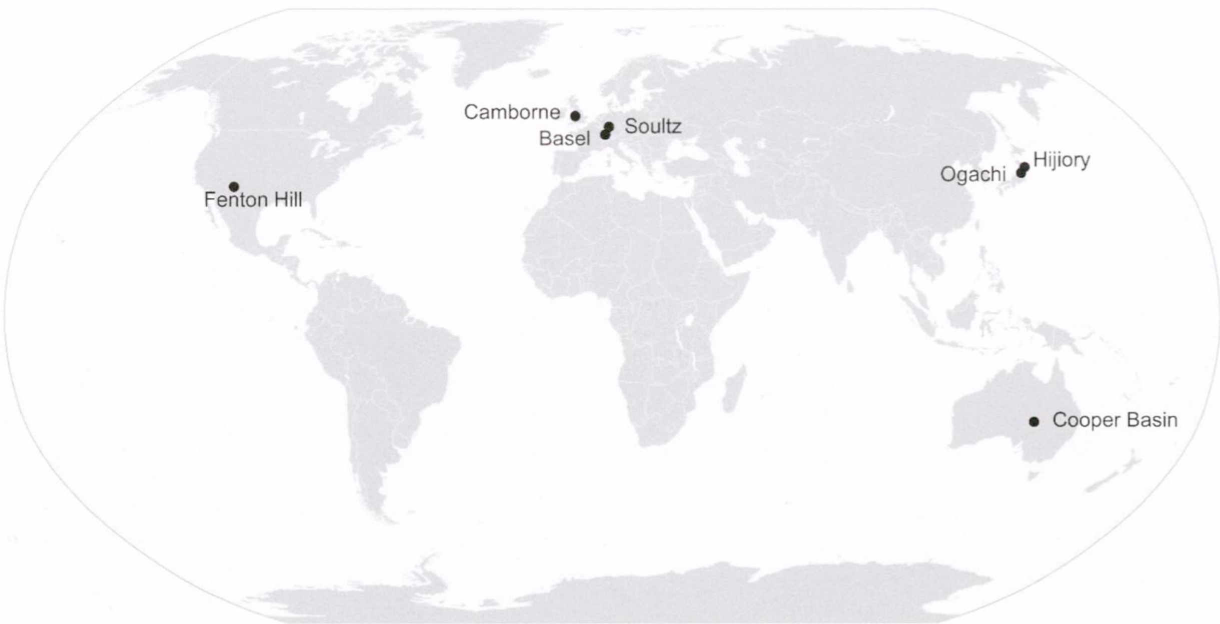

Fig. 2: Locations of the major international EGS-projects.

than 10 l/s to about 50 l/s. Only a few tests were done with flow rates above 100 l/s.
Basically two stimulation-schedules had been applied: the step-rate and the constant-rate injection schedule.

2.2 Example for a constant rate stimulation test

The basic idea behind the constant-rate stimulation schedule was to rise the pressure quickly to a high level so that fractures of various orientation could shear simultaneously. The test was performed in the open-hole section of borehole GPK4 in the Soultz II-system in the depth section between 4.500 m and 5.000 m. The aim was to hydraulically connect the well to the fracture system stimulated earlier in wells GPK2 and GPK3. The distance to the next well GPK3 was about 700 m. The test was started with about 600 m³ of brine followed by 8.500 m³ of water. The wellhead-pressure record shows the typical characteristics of a conventional hydraulic-fracturing test with a pressure maximum after start of injection (break-down pressure) and almost constant pressure until the end of injection (Fig. 3). During shut-in the pressure declined continuously without a sign of fracture closure.
The flow logs recorded during post-frac injection tests showed an almost linear decrease of the flow velocity with depth (Fig. 4). This is typical for axial fractures and is commonly observed after stimulating oil and gas wells in sedimentary rock formations. The logs indicate that the axial fracture extends over the entire length of the open-hole section accessible for logging. The high flow velocity at the lower end of the flow logs and the seismic cloud indicate that it extents further down to the bottom of the well and another 500 m beyond of it.
The seismic cloud was almost planar and was indicative for one through-going fracture. Dip and strike were vertical and N-S respectively. Stress conditions where transtensional with the maximum horizontal stress oriented 170° E. The great number and the character of the seismic signals, as well as the slight deviation of the strike direction from the direction of the maximum horizontal stress indicate that fracture propagation was not in a pure tensile mode but contained a shear-mode component.
These observations proof that large single

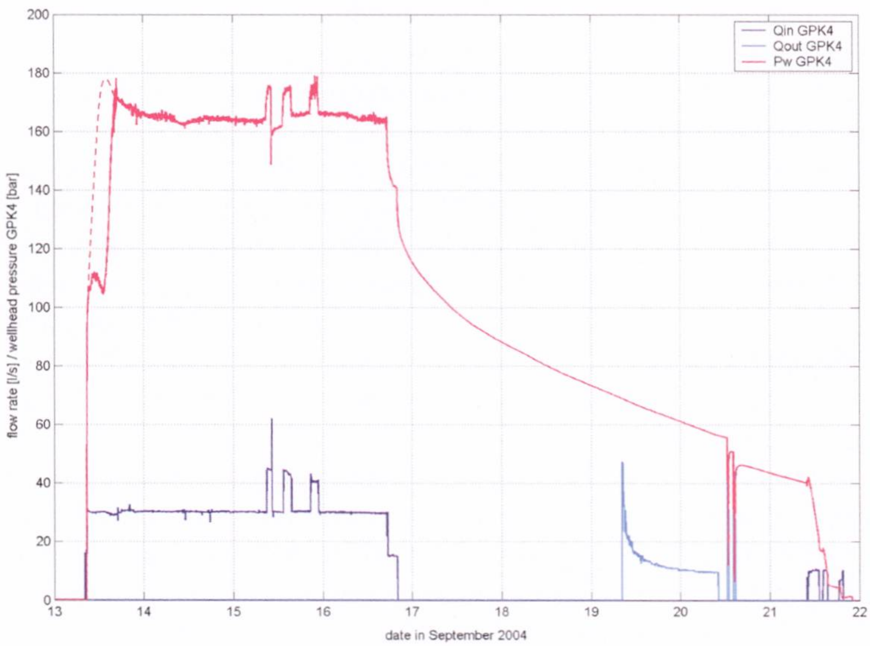

Fig. 3: Flow rate and wellhead-pressure record of a constant rate stimulation test in borehole GPK4 (Soultz II-system [Baria et al. 2005]). Dashed line in the pressure record: curve corrected for the density effect of brine injection.

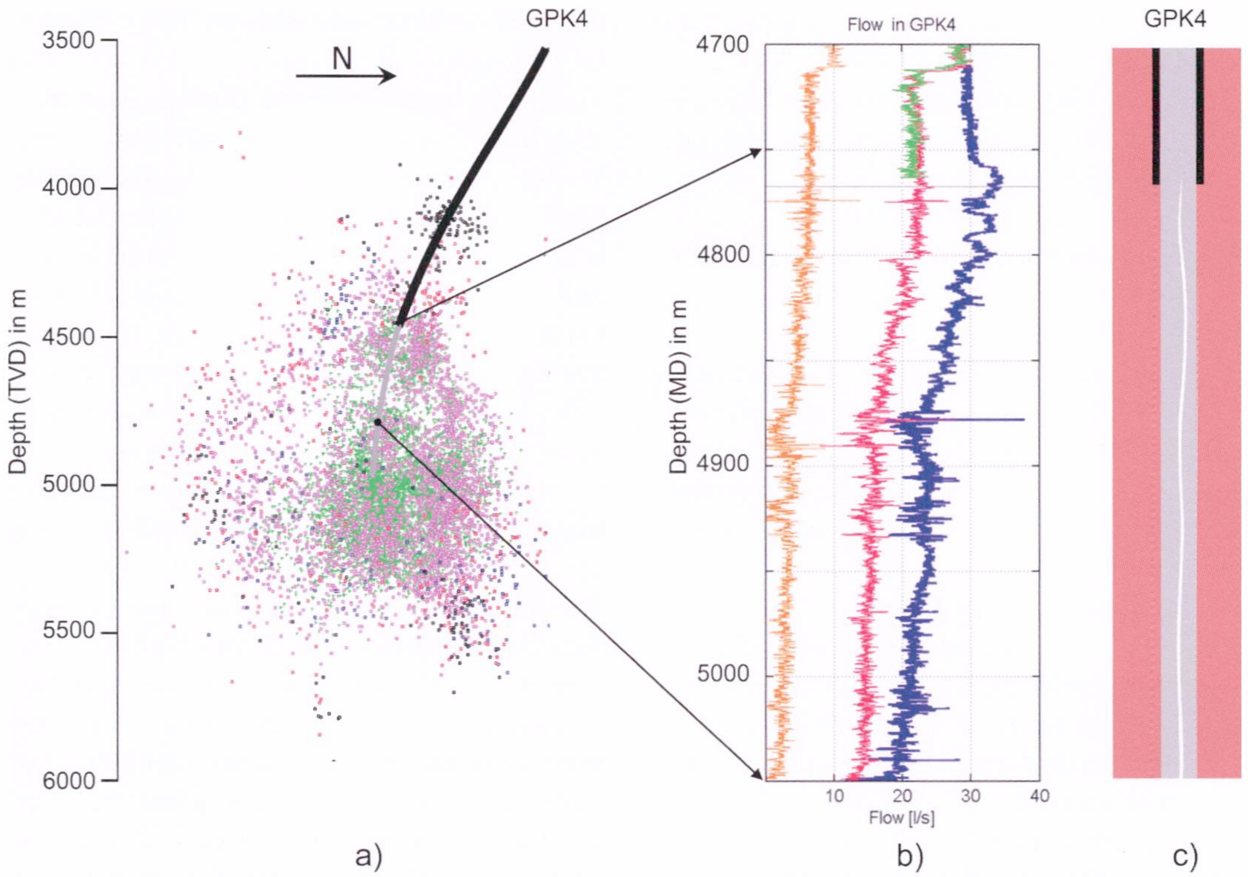

Fig. 4: Left: front-view of the seismic cloud of the stimulation test in borehole GPK4 of the Soultz II-system (view to the east), middle: flow logs recorded during post-frac injection tests, right: scheme of the fracture trace along the borehole wall (right). Sources: seismic cloud (Dyer 2005), flow-log (Schindler et al. 2008).

artificial fractures can be created by hydraulic stimulation in granite despite of the presence of hundreds of natural fractures. The presence of drilling induced axial fractures, the start of the stimulation at relatively high flow rates and an appropriate orientation of the borehole axis with respect to the stress field will favour the initiation of artificial fractures.

2.3 Example for a step-rate stimulation test

The rational of the step-rate stimulation tests was to first activate the fractures most ready for shearing and then activate step by step fractures less favourably oriented for shearing. The exemplary test was performed in the open-hole section of borehole GPK1 extending from 2.850 m to 3.400 m. It was the first stimulation test in the Soultz I-system. In order to isolate a permeable fault at about 3.500 m depth the bottom part of the well had been filled with sand. Starting flow-rate was 0.15 l/s, the maximum flow rate at the end of the test was 36 l/s (Fig. 5).

The pressure record did not show the typical characteristics of conventional hydraulic-fracturing tests described in the previous example. However the pressure reached a quite high level already during the first step and showed clear signs for a mechanical reaction from the beginning. The pressure increase from step to step was less than proportional to the flow rate steps and pressure remained almost constant for the final steps. This indicates that fractures had been jacked open at this pressure level. As for the constant rate test the pressure declined smoothly during the shut-in period before venting and showed no indication for fracture closure.

The seismic cloud of this test was processed with the so called «collapsing method» (Jones & Steward 1997). This method removes the random location error and leaves a more distinct image of the internal structure of the cloud. The front-view of the cloud (Fig. 6a) shows a quite complex internal pattern with a central patch and lines or stripes of intense seismicity, some of them radiating from the centre at different angles. In several directions the cloud has distinct almost straight boundaries. Views along the strike plane of the cloud as indicated in Fig. 6c and d, show a through-going structure resembling a large wing-crack. The overall strike direction of the vertical cloud is 155°. This is 15° off the direction of the maximum horizontal stress of 170°.

The step-like trace of intense seismicity in the horizontal slice as shown in Fig. 6b indicates that the lines of intense seismicity radiating from the centre are probably identical with the intersection lines of a vertical N-S striking fracture and some NNW-SSE-striking and ENE-dipping faults. It appears that the fracture is crossing them with a certain offset. The vertical fracture is most likely an artificial fracture created in the well section below the casing shoe that comprised a group of en-echelon drilling-induced fractures (Fig. 7). This fracture consumed or produced 60% of the fluid at the end of stimulation and during post-frac injection and production tests. Three deeper outlets absorbing another 25% of the flow rate were identified by Evans et al. (2005) as hydraulically linked to the main outlet below the casing shoe. This means that 85% of the injected fluid were flowing into the main fracture. The remaining 15% were absorbed by the permeable fault at 3.500 m depth after removing the sand and stimulating this lower part of the well. The pattern of the seismic cloud at this depth indicates that even this fault is connected to the main fracture. A more extensive analysis with a slightly dif-

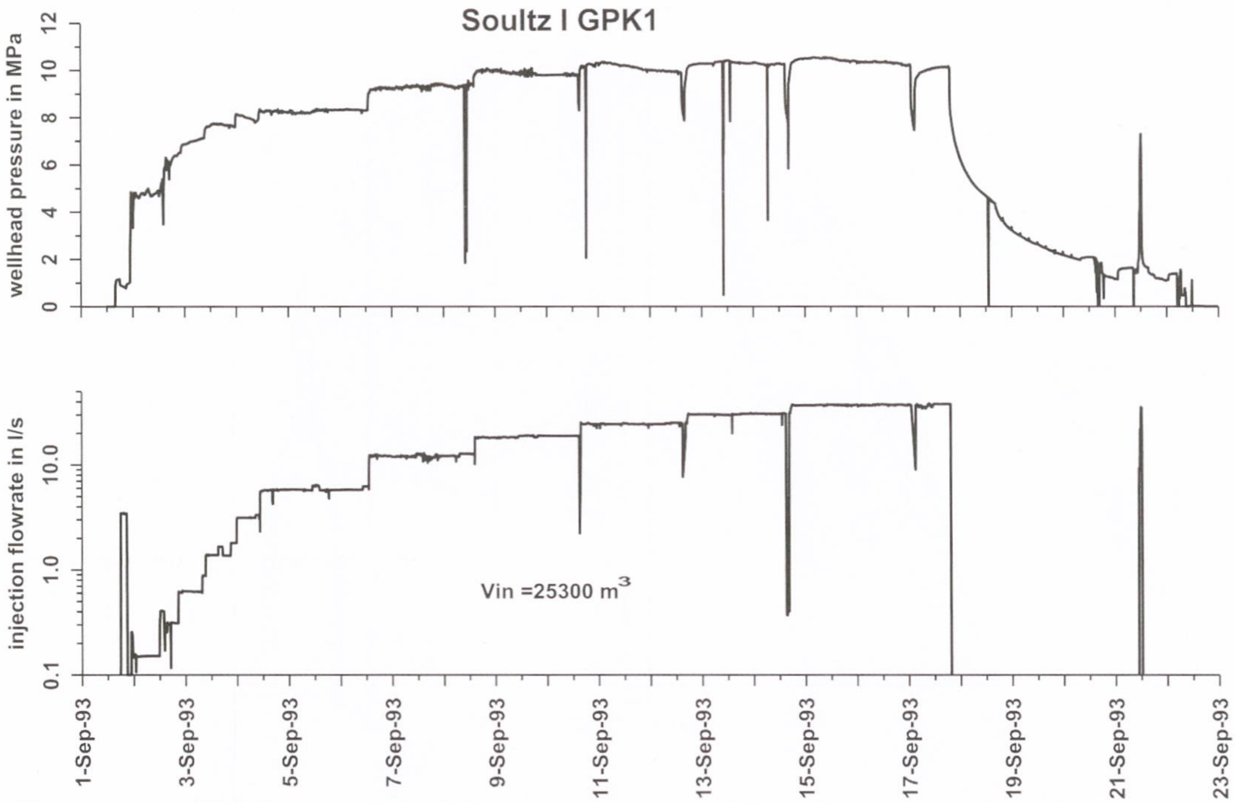

Fig. 5: Flow rate and wellhead-pressure record for the step-rate stimulation test in borehole GPK1 of the Soultz I-system. Note the logarithmic scale of the flow rate axis. Source: Jung (1999).

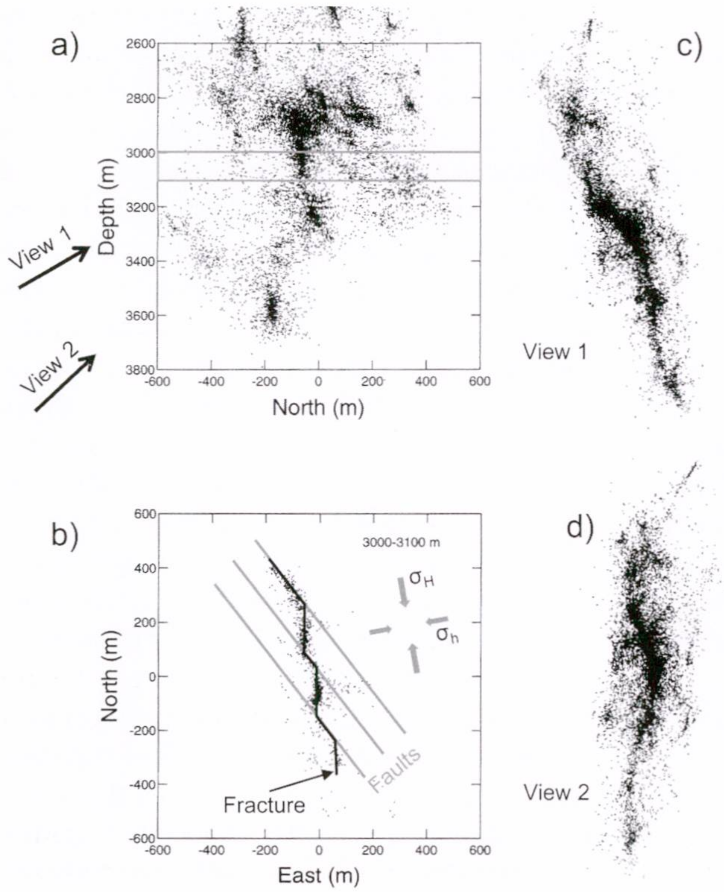

Fig. 6: Processed (collapsed) seismic cloud obtained during the step-rate stimulation test in borehole GPK1 of the Soultz I-system. a] front view (view toward W), b] horizontal slice (3.000– 3.100 m) c] & d] views parallel to the plane of a] along indicated directions. Source: Niitsuma et al. (2004).

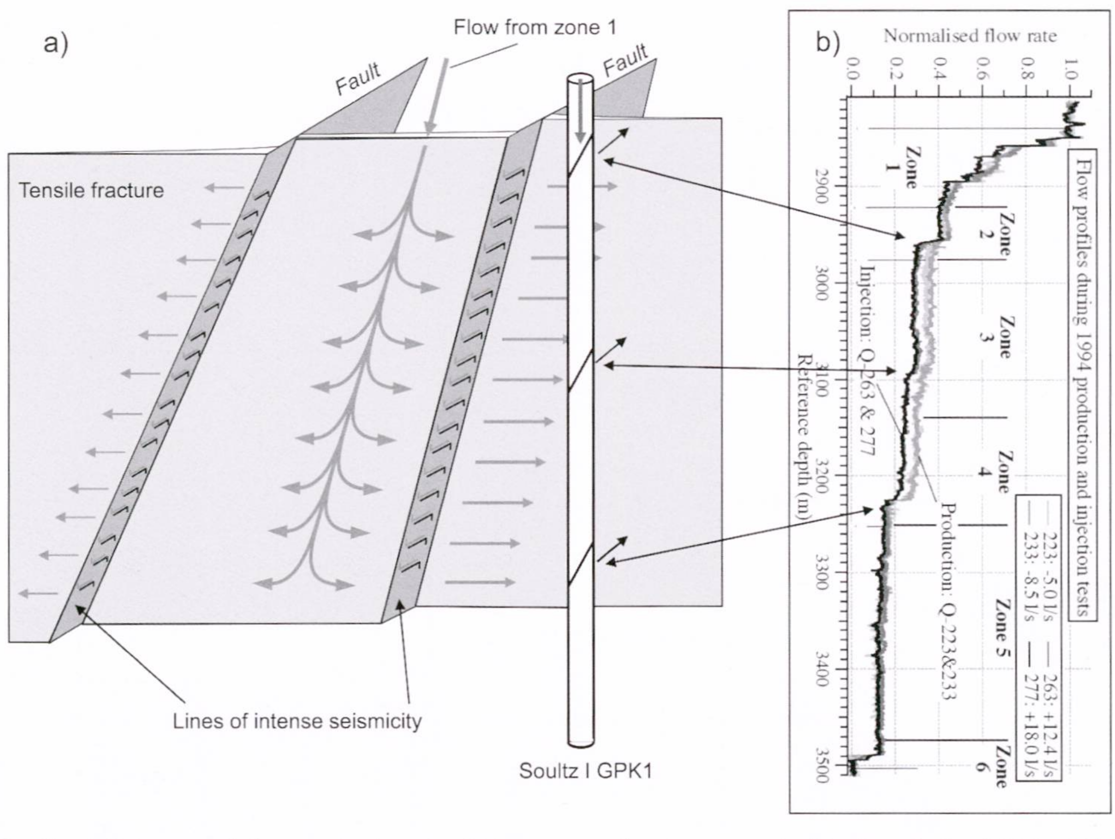

Fig. 7: a] Scheme of the central part of the macro-fracture created in borehole GPK1 of the Soultz I-system, derived from the flow logs and the seismic cloud (Fig. 6). b] flow-logs recorded during post-frac injection and production tests in borehole GPK1 at Soultz. Flow-log from Evans et al. (2005).

ferent interpretation of the seismic data was made by Evans et al. (2005).
In summary one can conclude that the step-rate stimulation test created a wing-crack-like macro-fracture that despite of intersections with faults is mechanically and most likely hydraulically a single large throughgoing entity.

3 General results and observations

Though the site- and test-conditions of the EGS-projects differed remarkably, an attempt was made to derive results and observations common to all EGS-systems. The only constants were rock type (granite and granodiorite) and frac-fluid (water or brine with one exception) and the fact that all tests were done in uncased borehole sections. All other test parameters and conditions were quite variable: Stress conditions ranged from normal- to thrust-faulting, depth from 800 m to 5.000 m (Fig. 8), temperature from 80 °C to 250 °C, length of frac-interval from 3 m to 750 m, injected volume from 20 m^3 to 35.000 m^3, and flow rates from 6 l/s to 200 l/s. Furthermore some tests were performed according to the constant-rate schedule, others according to the step-rate schedule. Well trajectories were predominantly vertical to sub-vertical but some tests (Los Alamos II and Camborne) were performed in inclined borehole sections.

3.1 Orientation of the stimulated fractures

It is generally assumed that tensile fractures are oriented perpendicular to the direction of the least compressive stress. Tensile fractures should therefore be vertical for normal and strike-slip stress conditions and horizontal for thrust-fault stress conditions. As mentioned above all basic stress conditions were covered by the major projects. Soultz had trans-tensional stress conditions which is the transition between normal and strike-slip stress conditions.
Investigation of the dip of the seismic clouds of the major EGS-projects showed that the seismic clouds were vertical to sub-vertical for strike-slip and trans-tensional stress conditions, steeply inclined (60–70°) for normal stress-conditions and subhorizontal for

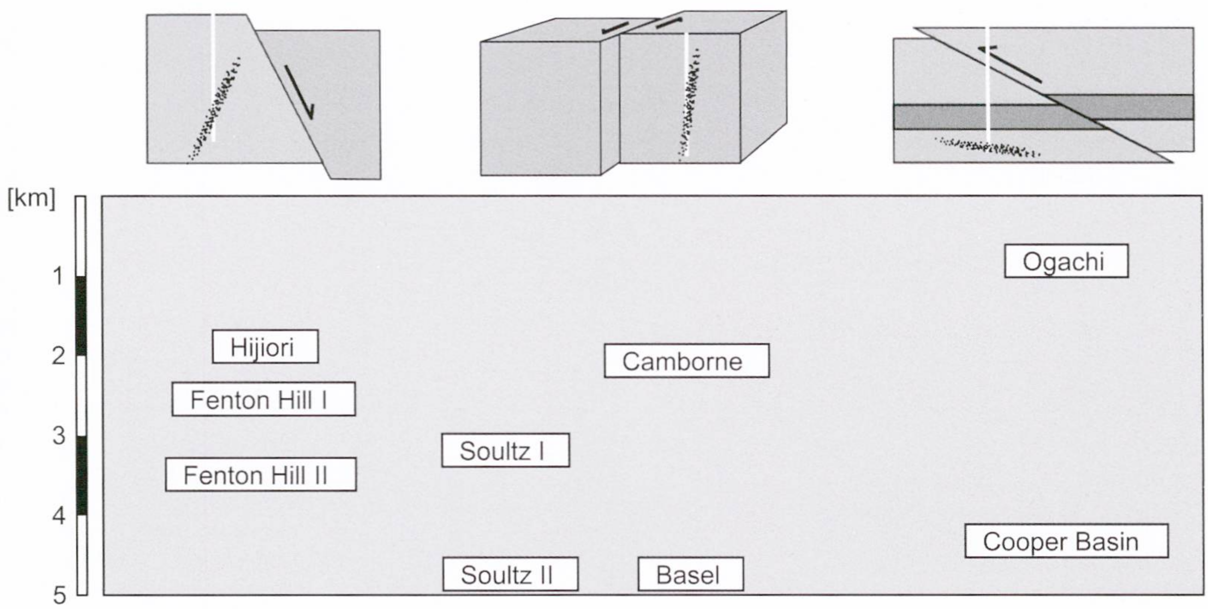

Correspondence of the dip of the seismic clouds with the stress conditions at the major EGS-sites. Scale on the left corresponds to the depth of the EGS-systems. (After Jung 2013).

thrust-faulting conditions (Jung 2013). This indicates that the dip of the stimulated fractures is similar to but not identical with the dip of tensile fractures. The biggest deviation is observed for normal stress conditions. In this case the dip of the fractures is optimal for shearing. For strike-slip conditions the strike of the fractures may also be optimal for shearing. But this was not proofed since there is often too high uncertainty in the direction of the principal horizontal stresses. In cases (e.g. Cooper Basin) it was suspected that the seismic cloud corresponds to a pre-existing fault that had been sheared during the stimulation tests. This argument cannot be disproofed but it seems unlikely that this is generally the case. One can therefore conclude that the tectonic stresses are the main controlling factor for the overall orientation of the stimulated fractures.

3.2 Size of the stimulated fractures

Because of the 2-dimensional nature of the seismic clouds and the strong influence of the location error on their thickness not the volume but the area of the seismic clouds was taken as the measure for the size of the stimulated fracture systems similar to an earlier study of Murphy et al. (1983). The area was grossly determined by drawing an envelope around the projection of the seismic clouds on a plane parallel to its main orientation.

Despite of the big variation in test and test-site conditions a clear correlation was found between seismic area and injected volume (Fig. 9). The whole set of data points except that of a gel-frac in the Camborne-project can well be fitted by a power law with exponent n = 2/3. This means that the area is increasing with $V_{IN}^{2/3}$. The area did not correlate with flow rate or length of the frac-interval (which could serve as a proxy for the number of natural fractures). These findings and the high coefficient of correlation R^2 of the data points with the fitting line allow establishing the following hypotheses:

- The stimulation process is mainly volume-controlled. Fluid losses have no significant impact. Fluid efficiency η (ratio of created fracture volume and injected volume) is high, at least in the order of 50%.
- Friction pressure losses in the fractures have no significant influence on the area to

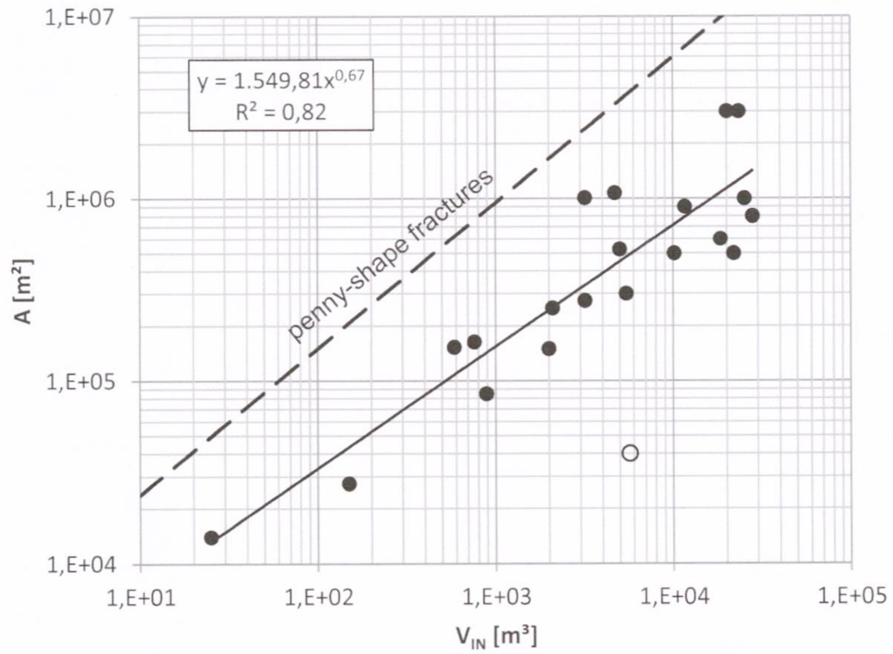

Fig. 9: Area of the seismic clouds of all major EGS-projects vs. injected volume (after Jung 2013). Fitting line and coefficient of determination R^2 is for the solid data points. Open circle: Data point of a gel-frac test in well RH-15 of the Camborne system. Dashed line: Trend-Line for penny-shape fractures for E´ = 50 GPa and K_{IC} = 1.5 MPa·m$^{1/2}$.

volume relationship. Static fracture models should therefore apply.

One of the most popular static fracture model is the circular tensile fracture, the so called «penny-shape fracture». Though it is clear that this model is not applicable for the stimulated fractures a comparison with this model is interesting. For the penny-shape fracture model, which neglects fluid-losses and the vertical stress gradient, the fracture-area is proportional to $V_{IN}^{0.8}$ and even more important it is by about one order of magnitude higher than the area of the seismic clouds (Fig. 9). The major technical consequence is that the fluid volume required for a certain fracture area is about ten times higher than the volume estimated with a penny-shape fracture model. Part of this big discrepancy may be explained by fluid-losses. But as mentioned above fluid losses played not an important role.

3.3 Number of stimulated fractures

Direct information on the number of conductive fractures was obtained from flow and temperature logging during stimulation and post-stimulation injection or production tests (Jung 2013). In no case was the number of hydraulically significant fractures bigger than five. Furthermore in most cases these fractures were close to each other and there was always a hydraulically dominating fracture among them. As demonstrated in the example above (Fig. 7) it is likely that some of the fractures are only hydraulic links to the main fracture since in most cases the main fracture stays close to the well over a long well section. It may therefore be concluded that the number of hydraulically significant fractures after stimulation was in all cases close to one.

3.4 Fracture aperture

Fracture apertures were determined with three independent methods, first by calculating the ratio of injected volume during stimulation and area of the seismic clouds, secondly by the tracer break-through volume observed during inter-well circulation tests, and third by using the hydraulic impedance measured during interwell circulation tests (Jung 2013).
The apertures determined by the ratio of

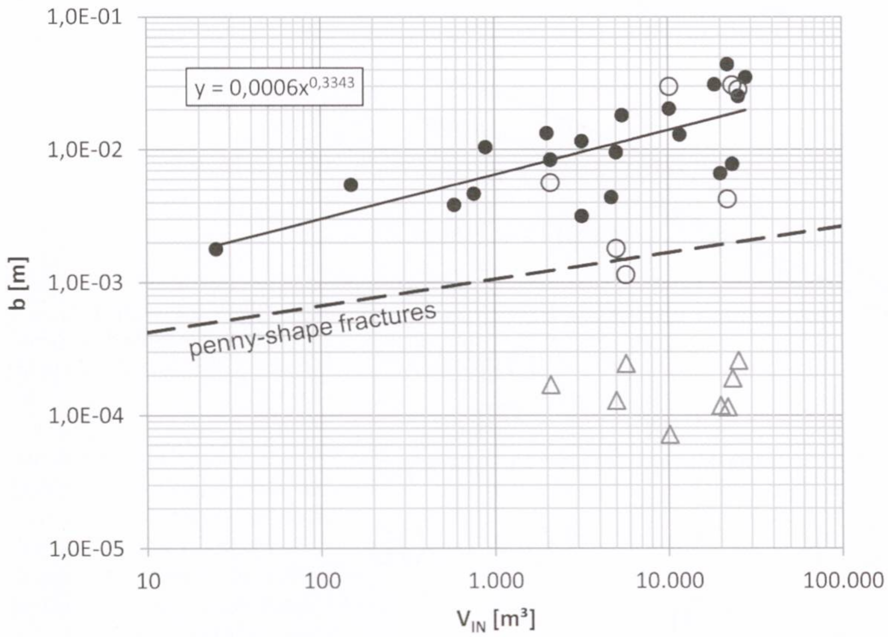

Fig. 10: Fracture apertures determined with different methods. Solid dots: ratio of the injected volume and seismic area, solid line: trend-line for the solid dots, open circles: apertures from tracer break-through volume, open triangles: apertures from hydraulic impedance, dashed line: trend-line for penny-shape fractures with K_{IC}= 1.5 MPa·m$^{1/2}$ and E´= 50 GPa, data from Jung (2013).

injected volume and area of the seismic cloud increase proportional with $V_{IN}^{1/3}$ and reach values of some centimeters for the largest fractures (Fig. 10). It is not surprising that the apertures determined this way are the highest since they are determined for propagating («inflated») fractures and since fluid losses are included. It is however surprising that most of the apertures determined from the tracer break-through volumes are close to these values. Even more striking is the fact that the apertures determined from the inter-well flow-impedance are by about two orders of magnitude lower than most of the values determined by the two other methods. This means that the hydraulic conductivity of the fractures (which is proportional to the cube of the aperture) are by about 6 orders of magnitude lower than the hydraulic conductivity that one would expect for the apertures determined by the two other methods. This could easily be explained when not a single fracture but multiple fractures were involved in the inter-well flow. But as the flow-logs have shown this was not the case.

3.5 Hydraulic characteristics of the fractures

Post-frac constant rate injection or production tests always showed a square-root or fourth-root of time-behaviour. This means the pressure in the test-well increases or decreases linearly with the square-root or fourth-root of time. In log-log-plots of the pressure and the logarithmic pressure-derivative this shows up as straight lines with slope ½ and ¼ respectively. Pressure-time curves of this type are characteristic for linear (parallel) flow within a fracture of finite hydraulic conductivity imbedded in an impermeable matrix (square-root of time behaviour) or in a permeable matrix (fourth-root of time behaviour). The square-root or fourth-root of time behaviour is commonly observed for hydraulic fractures in stimulated oil- or gas-wells but the duration of these periods particularly of the fracture linear flow-period is generally quite short. In the stimulated EGS-wells however fracture-linear flow-periods of 10 hours or more are not uncommon (Fig. 11). For axial fractures extending over several hundred meters along the borehole wall these long fracture-linear or bilinear flow-periods are reasonable. But the same behav-

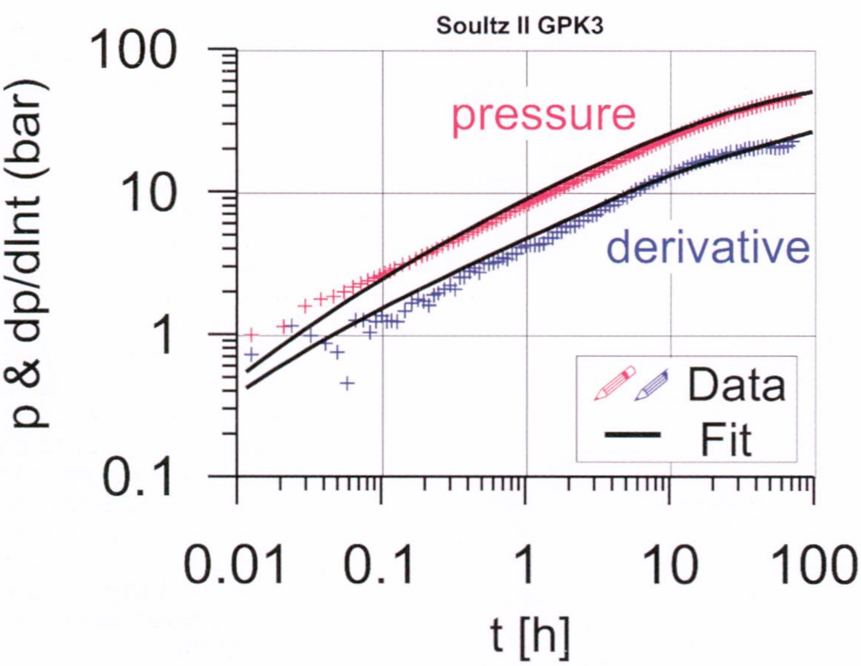

Fig. 11: Log-log-plot of the pressure (upper curve) and of the (logarithmic) pressure derivative vs. time of a post-frac constant-rate injection test at Soultz (Tischner 2013).

iour was also observed for fractures that had a point-like intersection with the borehole. In these cases the most plausible explanation is that the borehole is linked to a very long and highly conductive flow channel within the fractures, which acts as the baseline for the linear or bilinear fracture flow. Another or additional explanation is a strong anisotropy of the fracture-conductivity.
The hydraulic conductivity (transmissivity) of the fractures determined from the square-root or fourth-root of time-curves for single-well tests are in good agreement with the hydraulic impedance measured during inter-well circulation tests. Both values are most likely representative for the hydraulic conductivity normal to the orientation of the channels or normal to the axis of the highest fracture conductivity.

3.6 Thermal Draw-Down

The decline of the production temperature during circulation is the ultimate criterion for the success or the failure of an EGS-system and is a very sensitive indicator for the applicability of the models established for the EGS-system. Unfortunately only a few thermal-drawn curves of EGS-systems are available. In most cases the circulation tests were too short to obtain a thermal-draw down, or the test conditions were not well constrained.
The best examples concerning test conditions and test-duration are the thermal draw-down curves of the Los Alamos I and of the Camborne EGS-system (Fig. 12).
For both cases the temperature decline can well be fitted by single fracture models.

a [m]	260
b [m]	0,01
Q [m³/s]	0,015
T₀ [°C]	80,3
T_IN [°C]	20

A [m²]:	10000
b [m]	0,01
Q [m³/s]	0,006
T₀ [°C]	173
T_IN [°C]	25

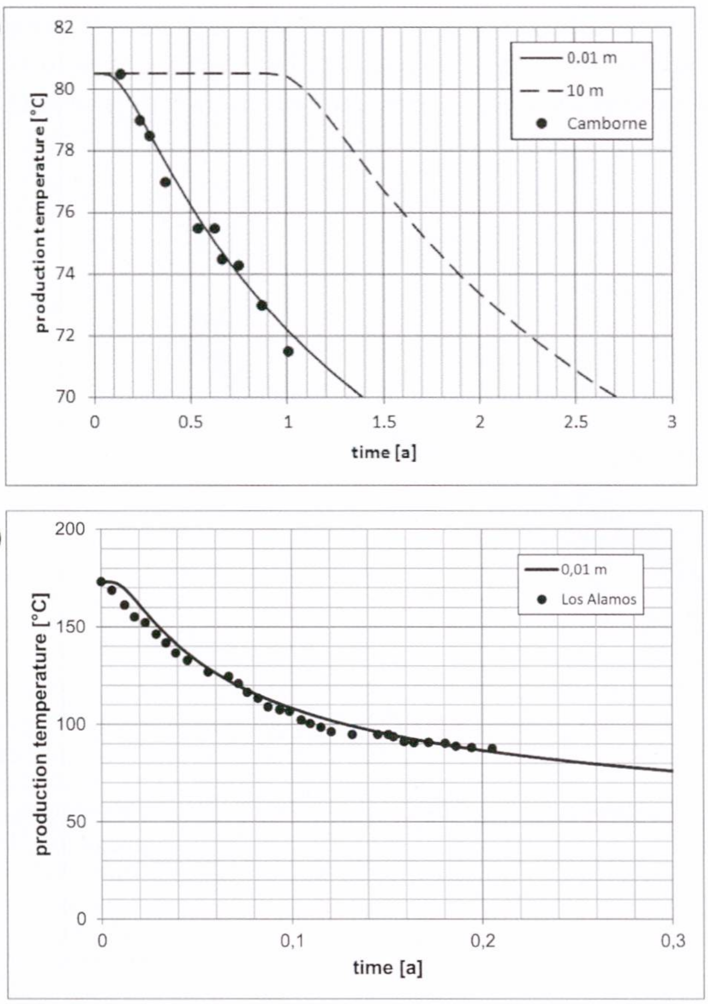

Fig. 12: Temperature decline during constant-rate circulation tests in Camborne II [a] and the Los Alamos I system [b]. Dots: data points, Solid lines: fit curves obtained with analytical single fracture models, dashed line: temperature decline for a doublet in a permeable layer with thickness b = 10 m. Data from Brown et al. [2012] and Ledingham [1989]. Tables: list of the parameter values used for fitting, a: inlet-outlet distance, b: fracture aperture, Q: flow rate, T_0: initial reservoir-temperature, T_{IN}: injection temperature, A: fracture area.

For the Los Alamos I system a good fit was found for a model with parallel fluid-flow in a rectangular fracture accompanied by transient conductive heat flow from the rock toward the fracture plane. The area of the fracture of 10.000 m^2 determined with this model agrees quite well with the value of 8.000 m^2 obtained with a similar model by the Los Alamos group (Brown et al. 2012) and corresponds with the inlet-outlet distance of about 80 m of this system.
For the Camborne-system a good fit was found by Ledingham (1989) by using a rectangular fracture model similar to the one above but comprising two fractures with flow-fractions of 79% and 21% respectively. A similar good fit (Fig. 12) is obtained with an analytical model that calculates the decline of the production temperature for a borehole-doublet in an infinite fracture with transient conductive heat flow from the rock matrix toward the fracture plane. The inlet-outlet distance of 260 m determined by using this model agrees quite well with the geometrical inlet-outlet distance of the Camborne-system (Tab. 2). If one replaces the discrete fracture in this model by a permeable layer with a thickness of several meters (a proxy for a volumetric system) the temperature decline starts with a significant delay as demonstrated in Fig. 12.
In summary one can conclude that both thermal draw-down curves can well be fitted by a single discrete fracture model. There is no indication for a volumetric or multi-fracture connection between the wells.

3.7 Induced Seismicity

All tests except the gel-frac test in the Camborne-project were accompanied by intense seismicity. The rate of seismic events was proportional to the flow rate but decreased gradually with time for constant flow rate. The number of detectable seismic events was generally in the order of one event per cubic-meter of injected volume. The source radius of the majority of events estimated from the frequency-characteristic (corner-frequency) was in the order of 5-10 m. A rel-

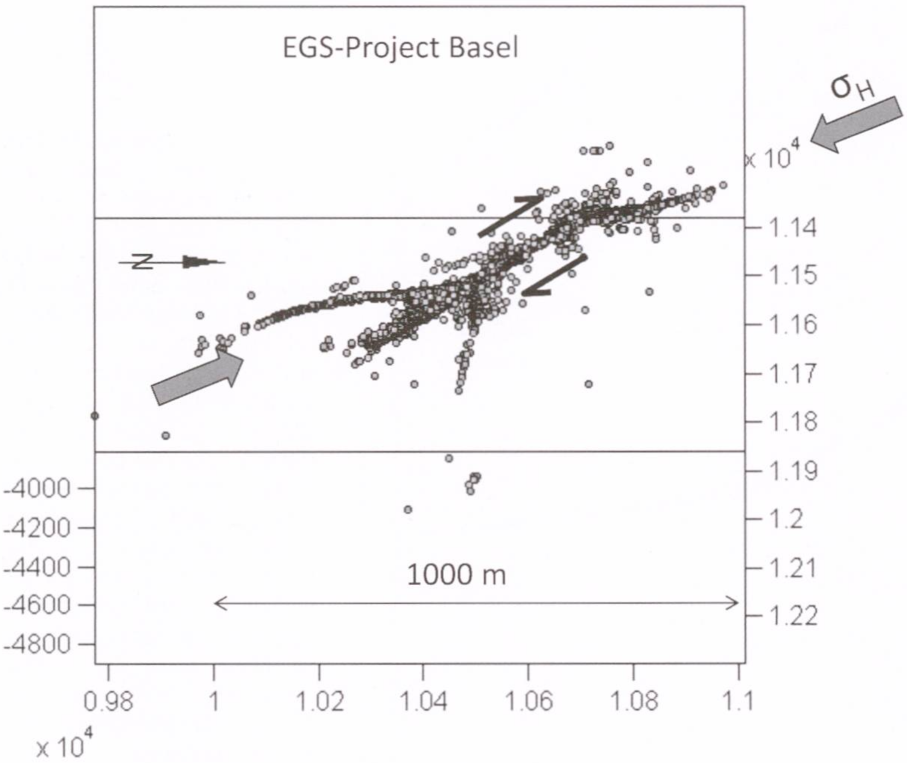

Fig. 13: Processed (collapsed) seismic cloud of the stimulation test in borehole BS-1 at Basel, view parallel to the central plane of the cloud (10° from vertical toward W). Processed Cloud from Baisch & Vörös (2007), stress-direction from Häring et al. (2008).

atively small fraction of events had much bigger source radii and magnitudes and appeared predominantly in the final part of the stimulation tests and during pressure depletion in the subsequent shut-in periods. In the Basel-system some strong events were observed several months after pressure depletion.

All seismic clouds of the major EGS-projects had a disk-like shape with a thickness of up to about 1 to 3 times the location error which was generally between 30 m and more than 100 m. Most of them had areas of intense seismicity in the central part surrounded by a halo of low seismicity. The transition between the two was abrupt and occurred in most cases along straight boundaries. The areas of intense seismicity were often elongated in one direction and in the extreme case almost linear. Similarly there were elongated patches and lines with no seismicity. Many of the regions in the inner part of the seismic clouds showed repeated seismicity. Subsequent stimulation tests in the same well produced almost no seismicity until the injected volume approached the injected volume of the initial test.

The generally diffuse appearance of the seismic clouds was to a main part due to the location error. When this was removed or reduced by applying appropriate processing methods like the so called «collapsing method» (Jones 1997) more distinct images of the fracture systems were produced giving insight into their internal structure. A number of these processed clouds showed the characteristics of a large wing-crack. The most obvious example besides the one in Fig. 6 is the seismic cloud of the Basel-system (Fig. 13).

4 Discussion

The present understanding of hydraulic stimulation as a pressure diffusion process in the natural fracture network accompanied by shearing and dilating of the natural fractures is based mainly on the fuzzy appearance of the seismic clouds, the strong shear wave components of the seismic signals, the great number of natural fractures encountered in granite even at great depth, and the onset of induced seismicity at a fluid pressure lower than the pressure required for the propagation of new tensile fractures.

Most of the results and observations described above however do not support this view. The small number of hydraulically significant fractures and the dominance of one in post-stimulation flow-logs, the rapid decline of the production temperature during circulation and the shape of processed seismic clouds indicate that mainly one trough-going macro-fracture is created during the stimulation process. This macro-fracture is oriented almost but not perfectly perpendicular to the direction of the minimum principal stress. At least for a number of cases the macro-fracture resembles a large wing-crack. On this basis it is hypothesized that the wing-crack mechanism plays a key role in the formation of these macro-fractures.

The formation of wing-cracks is one of the micro-mechanisms discussed in material science to explain the inelastic behavior and failure of brittle material under compression. The basic observation is that fractures of finite length failing in shear will not propagate along their own plane but will form tensile wing-fractures (Fig. 13). Referring to results of Coterell & Rice (1980), Lehner & Kachanow (1996) stated that the wings are initiated near the fracture tips at an angle of 70° to the plane of the initial shear fracture and are then bending into the direction of the maximum principal stress.

For natural fractures of the size of joints initiation of the wings start at a fluid pressure only a few bars above the pressure required for the onset of shearing. For natural fractures of a larger scale (fracture zones or faults) the difference is even smaller. This means that natural fractures being sheared during stimulation will inevitably develop wings. These wings will probably connect to neighboring fractures. The rising fluid-pressure within these fractures will cause them to shear and to develop wings at their tip. As a consequence a through-going fracture will develop consisting of natural and new fracture elements. It's orientation will be slightly off the direction of the maximum principal stress. When the pressure approaches the minimum principal stress large wing-fractures may develop at both ends of this series so that the whole fracture appears as a large wing-crack. It seems that most of the stimulated fractures at Soultz and the stimulated fracture of Basel are of this type. It is likely that the development of the large-scale wings are the reason for the strong seismic events in the final stages of these stimulation tests, since they enable large and simultaneous shear displacements of the whole series of natural and new fracture elements created earlier.

In long uncased borehole sections there are basically two different starting conditions for stimulation (Fig. 14). For step-rate stimulation tests stimulation will most likely start with the shearing of a natural fracture and the process will continue as described above. For constant rate stimulation tests with moderate to high flow rates an axial tensile fracture may be created. This tensile fracture will intersect natural fractures cause them to shear and to develop wings at their tips. The process will then continue as in the other case. For very high flow rates or viscous fluids the tensile fracture may cross the natural fractures before the fluid pressure had the time to migrate deeply into the natural fractures and to stimulate shearing. This crossing however happens generally with a certain offset at the interception. So also in this case the macro-fracture contains tensile fracture and natural fracture elements but probably with a smaller proportion of the latter.

In any of these cases the orientation of the macro-fracture is slightly off the direction of the maximum principal stress. As a consequence the maximum principal stress supports the propagation of the macro-fracture and enables fracture propagation at a fluid-pressure below the minimum principal stress.

For fluid flow in the macro-fracture the natural fracture elements act as resistors whereas the tensile fracture elements play the role of capacitors. Accordingly the hydraulic impedance of the macro-fracture is determined by the natural fracture elements whereas its aperture is determined by the tensile fracture elements. In three dimensions this pattern of natural and tensile fracture elements will most likely cause a strong anisotropy of the fracture conductivity with low conductivity parallel to the shear-direction and high conductivity perpendicular to it. Large wings at the tip of large natural frac-

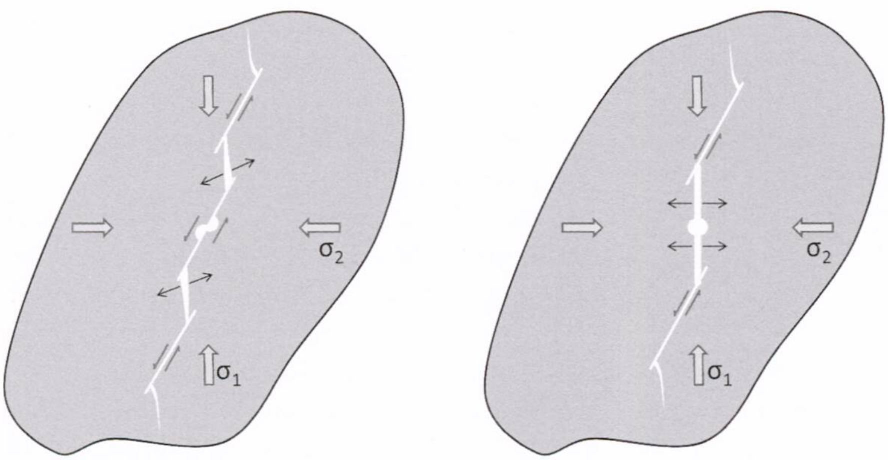

Fig. 14: Scheme of the two basic starting conditions for the evolution of a macro-fracture during hydraulic stimulation in fractured granite. Left: start by shearing of a natural fracture intersecting the well, right: start by creating an axial tensile fracture in the well.

tures or at the ends of a long series of natural and tensile fractures may form long through-going channels after pressure depletion.
During pressure depletion the tensile fracture elements will tend to close but at their roots they are hindered by the friction on the natural fracture elements. Big quantities of elastic energy are therefore temporary or permanently blocked near the roots of the tensile fractures, particularly of the large-scale wings. This energy may be set free explosively by sudden back-sliding of the natural fracture elements. This is a plausible explanation for the observation of strong events during the pressure depletion period and thereafter.
In summary the wing-crack model delivers plausible explanations for almost all observations described in the previous chapters in particular for: the onset of fracture propagation at a fluid pressure lower than the minimum principal stress, the high intensity and mechanism of induced seismicity, the occurrence of lines of intense seismicity in the seismic clouds, the long duration of the fracture-linear or bilinear flow periods during post-stimulation well tests, the occurrence of high magnitude events during and after pressure depletion, the large fracture apertures. It also explains the striking discrepancy between the only moderate fracture transmissibility and the large apertures. It seems therefore justified to use the wing-crack-model and the wing-crack-mechanism as a base for further investigations.

5 Summary and way forward

Observations and results of all major EGS-projects leave no doubt, that hydraulic stimulation cannot be regarded as merely a pressure diffusion process accompanied by shearing and dilating network of natural fractures. The data rather suggest that generally only one macro-fracture was created during the stimulation tests regardless of the flow rate and the length of the test interval or the number of natural fractures exposed to the fluid-pressure. These macro-fractures were steeply dipping for normal stress conditions, sub-vertical for strike-slip and trans-tensional conditions, and sub-horizontal for thrust-faulting stress conditions. Their area to volume ratio was much smaller than that of tensile fractures. The macro-fractures did not close after pressure depletion but retained a hydraulic conductivity suitable for inter-well flow rates between some l/s and about 25 l/s over well distances of up to 700 m. During single well hydraulic tests the fractures showed long fracture-linear or bilinear flow-periods indicating parallel flow within the fractures emerging from a long highly conductive flow-channel. All seismic events with magnitudes above the perceptible limit occurred in the final state of stimulation but also during or after pressure depletion. It is suspected that most of the macro-fractures created in the EGS-projects are wing-cracks and that the wing-crack mechanism is also acting on a smaller scale by linking adjacent natural fractures via fresh tensile fracture elements.
These findings suggest that the present EGS-concept will never lead to systems of industrial size and performance. It has to be abandoned and be replaced by a multi-fracture scheme as it was foreseen in the original Hot-Dry-Rock concept with the main difference that the tensile fractures of this concept have to be replaced by a type of macro-fractures consisting of natural and new tensile fracture elements. Fluid-flow in these macro-fractures is complex due to the presence of flow-channels and anisotropy of fracture conductivity. This poses risks but also offers the opportunity to maximize the heat exchanging area by a proper positioning of the second well.
Industrial systems of this type require wells being drilled parallel to the axis of the minimum principal stress, i.e. horizontal wells for normal and strike-slip stress conditions and vertical wells for reverse faulting condi-

tions. An industrial system may consist of about 30 to 40 equidistant fractures connecting two 1 km long parallel well sections with a well separation of about 500 m. Systems of these dimensions would operate for at least 25 years at flow rates of 100 l/s, an electric power output of 5 to 10 MW and a pumping power of less than 1 MW. Directional drilling and high temperature-packer technology have improved significantly during the last three decades (Shiozawa & McClure, 2014) and multi-fracture concepts are applied with great success in unconventional gas reservoirs. Though the conditions and requirements in geothermal applications are more demanding in various aspects it seems almost certain that geothermal multi-fracture systems of this type can be realized in the near future.

References

Baisch S. & Vörös, R. 2007: Personal Communication. Q-Con GmbH, Bad Bergzabern, Germany.

Baria, R., Michelet, S., Baumgärtner, J., Dyer, B., Nicholls, J., Hettkamp, T., Teza, D., Asanuma, H., Garnish, J., Megel, T., Kohl, T. & Kueperkoch, L. 2005: A 5000 m deep reservoir development at the European HDR Site at Soultz. Proc. 30th Workshop on Geothermal Reservoir Engineering, Stanford Univ., Stanford, Cal., Jan. 31 – Feb. 2.

Batchelor, A. S. 1982: The creation of Hot Dry Rock systems by combined explosive and hydraulic fracturing. Proceedings of the International Conference on Geothermal Energy, May 1982. Florence, Italy. BHRA Fluid Eng. Bedford, 321–342.

Brown, D. W., Duchane, D. V., Heiken, G., Hriscu, V. T. 2012: Mining the earth´s heat: Hot Dry Rock geothermal energy. Springer-Verlag, Berlin Heidelberg, ISBN 978-3-540-67316-3, DOI 10.1007/978-3-68910-2.

Cornet, F. H. 1989: Experimental investigations of forced fluid flow through a granite rock mass. Proceedings of 4th Int. Seminar on the results of EC Geothermal Energy Demonstration, Florence, Italy, April 27-30, 1989, 189–204.

Cotterell, B. & Rice J. R. 1980: International Journal of Fracture 16. 155–169.

Dreesen, D. S. & Nicholson R. W. 1985: Well completion and operations for the MHF of Fenton Hill HDR Well EE-2. Proceedings Geothermal Resources Council, Kailua-Kona, Hawaii, Aug. 26–30, 1985.

Dyer, B. C. 2005: Soultz GPK4 stimulation September 2004 to April 2005 – Seismic monitoring report. Seamore Seismic, Falmouth, Cornwall, UK.

Evans, K. F., Moriya, H., Niitsuma, H., Jones, R. H., Phillips, W. S., Genter, A., Sausse, J., Jung, R. & Baria, R. 2005: Microseismicity and permeability enhancement of hydro-geologic structures during massive fluid injections into granite at 3 km depth at the Soultz HDR site. Geophys. J. Int., 2005, 160, 388–412.

Häring, M. O., Schanz, U., Ladner, F. & Dyer B. C. 2008: Characterization of the Basel1 Enhanced Geothermal System. Geothermics, 2008. doi:10.1016/j.geothermics.2008.06.002.

Hayashi, K. & Abé, H. 1989: Evaluation of hydraulic properties of the artificial subsurface system in Higashihachimantai geothermal model field. J. Geothermal Research Soc. Japan, Vol. 11, No. 3, 203–215.

Jones, R. H. & Stewart, R. C. 1997: A method for determining significant structures in a cloud of earthquakes. J. geophys. Res. 102, 8245–8254.

Jung, R. 1989: Hydraulic In Situ Investigations of an Artificial Fracture in the Falkenberg Granite. Int. J. Rock Mech. Sci. & Geomech. Abstr. Vol. 26, No. 3/4, 301–308.

Jung, R. 1999: Erschliessung permeabler Risszonen für die Gewinnung geothermischer Energie aus heissen Tiefengesteinen. Schlussbericht BMBF-Forschungsvorhaben 0326690A, Bundesanstalt für Geowissenschaften und Rohstoffe, Hannover, Archiv Nr. 118977, S. 38.

Jung, R. 2013: EGS – Goodbye or back to the future. In: Effective and Sustainable Hydraulic Fracturing, A. P. Bunger, J. McLennan & R. Jeffrey (eds.), 95–121, InTech, doi:10.5772/45724.

Ledingham, P. 1989: Circulation results 1983–1986. In R. H. Parker (ed.), Hot Dry rock geothermal Energy, Phase 2B final report of the Camborne School of Mines Project, Vol. 1, Pergamon Press, Oxford UK, 388–408.

Lehner, F. & Kachanov, M. 1996: Modelling of «winged» cracks forming under compression. International Journal of Fracture 77, 1996, R69–R75.

MIT 2006: The Future of Geothermal Energy – Impact of Enhanced Geothermal systems (EGS) on the United States in the 21st Century. Idaho Nat. Lab., Idaho US, http://geothermal.inel.gov.

Murphy, H. 1985: Hot Dry Rock phase II reservoir engineering. Los Alamos Nat. Lab. Rep. LA-UR-85-3334.

Murphy, H., Keppler, H. & Dash, Z. 1983: Does hydraulic fracturing theory work in jointed rock masses?. Geothermal Resources Council, Transactions Vol. 7, Oct. 1983, 461–466.

Niitsuma, H., Asanuma, H. & Jones, R. 2004: personal communication, Tohoku University, Sendai Japan & Camborne School of Mines, Redruth Cornwall UK.

Rowley, J. C., Pettitt, R. A., Matsunaga, I., Dreesen, D. S., Nicholson, R. W. & Sinclair, A. R. 1983: Hot-Dry-Rock Geothermal reservoir fracturing initial field operations – 1982. Proceedings Geothermal Resources Council 1983 Annual Meeting, Oct. 24-27, Portland, Oregon US.

Schindler, M, Nami, P., Schellschmidt, R., Teza, D. & Tischner, T. 2008: Summary of hydraulic stimulation operations in the 5 km deep cystalline HDR/EGS reservoir at Soultz-sous-Forêts. Proc. 33rd Workshop on Geothermal Reservoir Engineering, Stanford Univ., Stanford, Cal., Jan. 28–30, 2008.

Shiozawa, S. & McClure, M. 2014: EGS Designs with Horizontal Wells, Multiple Stages, and Proppant. Proc. 39th Workshop on Geothermal Reservoir Engineering, Stanford Univ., Stanford, Cal., Feb. 24–26.

Tischner, T. 2013: personal communication, Bundesanstalt für Geowissenschaften und Rohstoffe, Hannover.

Wallroth, T. 1992: Hydromechanical breakdown of crystalline Rock. Publ. A 71, Diss., Chalmers Tekniska Högskolar, OCH Göteborgs Universitet, Sweden.

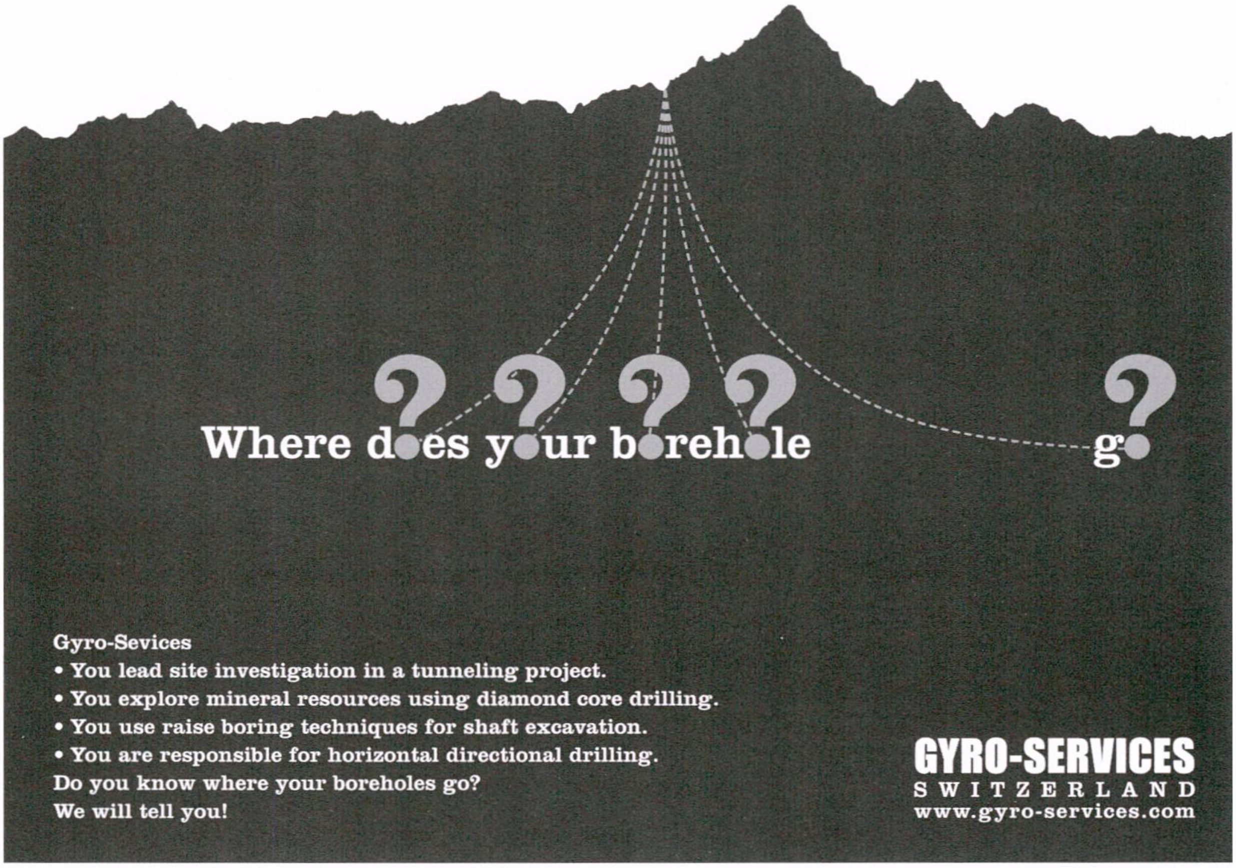
Where does your borehole go?
Gyro-Sevices
• You lead site investigation in a tunneling project.
• You explore mineral resources using diamond core drilling.
• You use raise boring techniques for shaft excavation.
• You are responsible for horizontal directional drilling.
Do you know where your boreholes go?
We will tell you!
GYRO-SERVICES
SWITZERLAND
www.gyro-services.com